肌动蛋白结合蛋白Anillin通过靶向细胞核中的c-Myc介导上皮–间质转化并促进胃癌进展

符明诗[1] 史珂[1] 刘东洋[2] 陈风[2]*

([1]上海海洋大学水产与生命科学学院, 上海 201306; [2]上海第六人民医院普外科, 上海 200233)

摘要 肌动蛋白结合蛋白(ANLN)在细胞增殖和迁移中起重要作用, 特别是在胞质分裂中。虽然已有研究结果表明癌症的发生发展与ANLN有关, 但其影响胃癌(GC)发生发展的潜在调控作用和分子机制仍不清楚。在此, 先采用伤口愈合实验、Trans-well实验和基质(Matrigel) Trans-well实验检测ANLN表达情况对体外胃癌细胞迁移和侵袭能力的影响。然后, 采用免疫印迹实验来评估上皮–间充质转化(EMT)相关蛋白和Smad蛋白的表达。此外, 还采用共定位免疫荧光法、免疫共沉淀法(Co-IP)和Western blot探索ANLN参与胃癌转移的分子机制。在此研究中, 沉默*ANLN*减弱了胃癌细胞的迁移和侵袭能力。在机制上, ANLN可以与细胞核中的c-Myc 相互作用, 随后c-Myc 发生磷酸化, 诱导Snail和Slug转录因子的表达, 促进EMT, 但不激活Smads蛋白。总的来说, 该文的数据揭示了一个潜在的分子机制, 即ANLN通过分别介导Smads信号通路和c-Myc 蛋白进而靶向调控下游转录因子(Snail和Slug)触发EMT进程。

关键词 肌动蛋白结合蛋白(ANLN); 胃癌(GC); c-Myc; 上皮–间质转化(EMT); Smads

Anillin Mediates EMT by Targeting c-Myc in the Nucleus and Potentiates Gastric Carcinoma Progression

FU Mingshi[1], SHI Ke[1], LIU Dongyang[2], CHEN Feng[2]*

([1]*College of Fisheries and Life Science, Shanghai Ocean University, Shanghai 201306, China*;
[2]*Division of General Surgery, Shanghai Jiao Tong University Affiliated Sixth People's Hospital, Shanghai 200233, China*)

Abstract ANLN (Anillin), an actin-binding protein, reportedly plays a vital role in cell proliferation and migration, particularly in cytokinesis. Although there have been findings pointing to a contribution of ANLN to the development of cancer, the potential regulatory roles and molecular mechanisms by which ANLN affects the development and progression of GC (gastric carcinoma) remain obscure. Herein, applying wound healing assay, Trans-well migration and Matrigel Trans-well assays to detect the effect of ANLN expression on migration and invasion ability of GC cells *in vitro*. Then, performing Western blot to evaluate EMT (epithelial-mesenchymal transition) associated proteins and Smad proteins. Moreover, performing immunofluorescence assay, Co-IP (co-immunoprecipitation) assay and Western blot to explore molecular mechanisms by which ANLN is involved in GC metastasis. In this study, *ANLN* silencing attenuated GC cell migration and invasion. Mechanistically, ANLN could interact with c-Myc in the nucleus and subsequently phosphorylate c-Myc to induce the expression of Snail and Slug transcrip-

收稿日期: 2021-12-26 接受日期: 2022-03-21
上海医药卫生大学国家培养计划项目(批准号: SFP-18-20-14-005)和上海市浦东新区科技发展基金(批准号: PKJ2016-Y54)资助的课题
*通讯作者。Tel: 18930174853, E-mail: sd_chenf@sumhs.edu.cn
Received: December 26, 2021 Accepted: March 21,2022
This work was supported by the National Cultivation Project of Shanghai University of Medicine & Health Sciences (Grant No.SFP-18-20-14-005), and the Technology Development Foundation of Pudong District (Grant No.PKJ2016-Y54)
*Corresponding author. Tel: +86-18930174853, E-mail: sd_chenf@sumhs.edu.cn

tion factors, to promote EMT but does not activate Smad proteins. Collectively, the data reveal a potential molecular mechanism in which ANLN mediates Smads signaling pathway and c-Myc protein respectively, which target downstream transcription factors (Snail and Slug) to trigger EMT.

Keywords ANLN (Anillin); GC (gastric carcinoma); c-Myc; EMT (epithelial-mesenchymal transition); Smads

GC (gastric carcinoma) is one of the most common cancers and causes of cancer death worldwide [1-2]. More than four-fifths of patients with GC are diagnosed in the middle and late stages because the symptoms are not obvious [3]. The 5-year survival rate of global GC patients is less than one-fifth [4]. Therefore, the molecular mechanism of the occurrence and development of GC is currently the focus of research.

ANLN (Anillin) is an actin binding protein that has been documented as a key factor in cell division, and it is a multi-domain protein that interacts with many proteins [5]. ANLN is highly expressed in many types of site-specific cancerous tumors and involves in cancer progression [6-12].

To date, Myc and ANLN have been discovered to interact through experimental evidence, including affinity capture-MS [13], and proximity label-MS [14] and curated by the Biogrid [15]. The Myc family of oncogenes (*c*-, *N*-, and *L-Myc*) encodes a set of transcription factors that feature prominently in cancer [16]. Myc protein acts as both a transcriptional activator and a transcriptional suppressor, and plays a role in tumor initiation by controlling the expression of thousands of genes involved in cell growth, proliferation, metabolism and genomic stability [17]. MAX, the chaperone of Myc, creates a stable DBD (DNA-binding domain) for Myc's recognition of target genes, which recognizes the E-box motifs (CACGTG) in promoters and enhancer of Myc regulatory genes [18]. Once bound to its target sites, Myc interacts with sets of cofactors to modulate the gene expression patterns that ultimately lead to malignancy [18-20]. These results prompted us to test whether the interaction between ANLN and c-Myc is involved in GC metastasis.

EMT, a complex cellular pathway in which epithelial cells lose cell-to-cell adhesion (characterized by membranous E-Cad loss) and gain mesenchymal characteristics (characterized by increased N-cadherin expression and migratory capabilities), is not only critical in development and wound healing, but also represents a salient property of primary tumor formation and metastasis [21]. Transcription factors play an important role in the process of EMT. Currently, it has been reported that EMT-related transcription factors include Snail family, ZEB (zinc finger E-box-binding) protein family, and bHLH (basic helical-loop-helical protein) homodimers and heterodimers [22-28].

In this study, *ANLN* down-regulation stably significantly impaired metastasis of GC cells. Furthermore, our study revealed a possible molecular mechanism by which ANLN mediates independent Smads and c-Myc signaling pathways, triggering EMT by targeting Snail and Slug downstream transcription factors.

1 Materials and methods

1.1 Antibodies and reagents

E-cadherin, N-cadherin, Vimentin, Snail (Slug), MMP2, MMP9, ANLN, p-c-Myc (S62), c-Myc and β-actin antibodies were purchased from Abcam (Cambridge, MA, USA). The inhibitor 10058-F4 was obtained from Beyotime (Shanghai, China). The Alexa Fluor 488- and 594-conjugated secondary antibodies were obtained from Abcam (Cambridge, MA, USA).

1.2 Cell culture

MGC-803 cells were originally obtained from the Shanghai Institute of Life Sciences at the Chinese Academy of Sciences (Shanghai, China). MGC-803 cells were incubated in RPMI-1640 medium containing 10% fetal bovine serum, 100 U/mL penicillin and 100 mg/mL streptoMyc in, and then cultured in a 5% CO_2 humidification atmosphere at 37 ℃, and cells between the third and tenth passages were used in this study.

1.3 Generation of stable cell lines

MGC-803 cell line that stably expressed *ANLN* shRNA or control-shRNA were constructed using a

lentiviral shRNA technique. Oligonucleotides were constructed in the pLent-U6-GFP-Puro vector (Vigene Biosciences, USA). PuroMyc in (6 μg/mL) was used to select for stably transfected cells for 4 weeks. The human *ANLN* shRNA sequence was designed as follows: 5′- GCT CTG ACA TTC ACT ACT ATT CAA GAG ATA GTA GTG AAT GTC AGA GCT TTT TTT-3′.

1.4 Wound-healing assay

Adding about 5×10^5 cells to the 6-well plate, and scraping the fused monolayers into straight lines with a sterile 1 000 μL plastic straw tip. Un-adherent cells were removed with sterile PBS and then replaced with fresh serum-free medium. After incubation for 24 h, wound photos were taken with an inverted microscope (Leica, Germany).

1.5 Trans-well migration assay

100 μL of a cell suspension (5×10^4 cells) in serum-free medium was added to the upper compartment of the Trans-well migration chambers (BD, USA). The bottom chamber was filled with 600 μL of medium containing 10% fetal bovine serum. After a 24 h incubation period, cells were fixed with 100% methanol for 30 min and stained with 0.1% crystal violet for 20 min. The number of cells that penetrated the membrane were counted in five random fields.

1.6 Matrigel Trans-well assay

The upper compartments of the Trans-well migration chambers (BD, USA) were precoated with 80 μL of Matrigel at 4 ℃ overnight. 100 μL of cell suspension (5×10^4 cells) in serum-free medium was added to the upper compartment of the Trans-well migration chambers (BD, USA). The bottom chamber was filled with 600 μL of medium containing 10% fetal bovine serum. After incubation at 37 ℃ for 24 h, cells were fixed with 100% methanol for 30 min and stained with 0.1% crystal violet for 20 min. The number of cells that penetrated the membrane were counted in five random fields.

1.7 Co-IF (co-location immunofluorescence) assay

Cells (3×10^5) treated with or without 20 μmol/L 10058-F4 were grown on glass coverslips in 24-well plates for 24 h. The cells were fixed and permeated and then closed, next were incubated overnight with diluted primary antibody at 4 ℃. Fluorescence secondary antibody incubation and DAPI redye nuclei were carried out in the dark, and Co-IF (co-location immunofluorescence) images of the indicated proteins were acquired with an inverted microscope.

1.8 Western blot

RIPA buffers lysed cells and BCA protein detection kit (Beyotime, Shanghai, China) measured protein concentrations. Proteins were separated by SDS-PAGE and then transferred to the PVDF membrane. Next, QuickBlock™ Blocking Buffer (Beyotime, Shanghai, China) blocked the membranes for 15 min at 25 ℃. Then incubated overnight with primary antibodies at 4 ℃ and secondary antibody for 1 h. Signals were examined using the ECL chemiluminescence reagent on the electrochemiluminescence system (Bio-Rad Laboratories, Hercules, CA).

1.9 Co-IP (co-immunoprecipitation) assay

Cells at 90% confluence were lysed in IP lysis buffer containing protease inhibitors and precleared with protein A-, G-Sepharose beads for 60 min. The lysates were then incubated overnight with primary antibody or non-specific IgG (immunoglobulin) in the presence of protein A- and G-agarose beads. Rinsed beads with 40 μL cold elution buffer. Then, 30 μL of 5× sample buffer was added to the eluted samples followed by boiling at 95 ℃ for 5 min. The expression of the expressed protein was analyzed by Western blot.

1.10 Statistical analysis

Statistical analysis was performed using Excel. All data were expressed as means±standard error of the mean (s_x) obtained from at least three independent experiments. The two groups of independent samples were compared by two-tailed student *t* test. Multiple comparisons were performed using One-Way analysis of variance. Significant differences were as follows: $^*P<0.05$; and $^{**}P<0.01$.

2 Results

2.1 ANLN is abnormally overexpressed in GC cells and is associated with prognosis of GC

A previous study showed that ANLN is aberrantly overexpressed in GC and positively correlated with GC progression [29], we adopted Kaplan Meier-Plotter

(http://kmplot.com/analysis/) online tool to analyze the relationship between ANLN and the prognosis of GC. The median expression level of ANLN was used as the basis for grouping, and the patients were divided into high and low expression groups. Then, the OS (overall survival) of GC was selected for analysis. The results showed that ANLN expression level was negatively correlated with prognosis of patients (Fig.1A). To confirm ANLN overexpression in GC, we determined the expression of ANLN in two GC cell lines (SGC-7901 and MGC-803), and normal gastric cell line (GES-1). Western blot assay showed that levels of ANLN protein in GC cell lines (SGC-7901 and MGC-803) were higher than normal gastric cell line (GES-1) (*P<0.01) (Fig.1B). For the next experiment, lentivirus vector plasmid of pLenti-shRNA-*ANLN* and pLenti-shRNA-NC lentivirus vector were transfected into MGC-803 cells respectively to construct sh-*ANLN* experimental group and negative control group sh-NC group. RT-PCR and Western blot showed that stable transfection efficiency was statistically significant (*P<0.05) (Fig.1C and Fig.1D).

2.2 Depletion of *ANLN* suppresses the metastasis of MGC-803 cells *in vitro*

To determine whether knockdown of *ANLN* expression affected MGC-803 human GC cells migra-

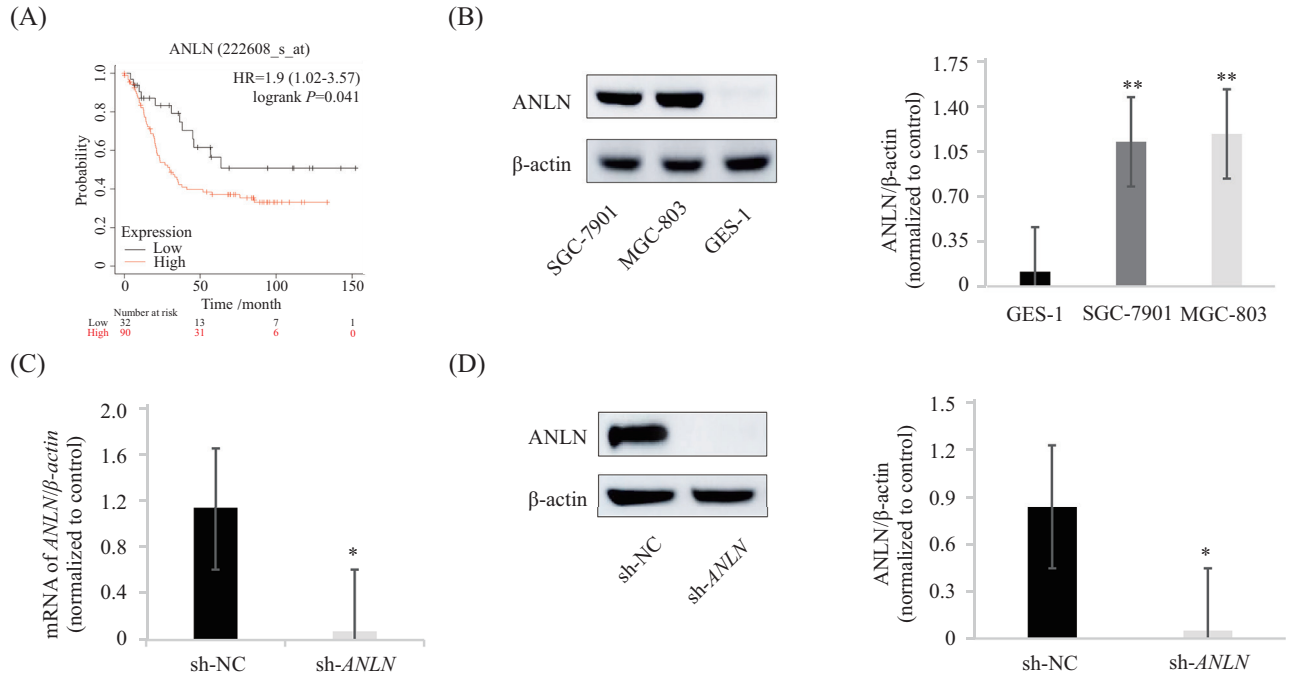

A: 胃癌患者中ANLN过表达与生存率呈负相关, 总生存期(OS)分析; B: 通过Western blot分析SGC-7901、MGC-803和GES-1细胞系中ANLN的表达水平, **P<0.01, 与GES-1组相比; C: 实时PCR分析, 将pLenti-shRNA-*ANLN*和pLenti-shRNA-NC慢病毒载体分别转染MGC-803细胞分别作为实验组(sh-*ANLN*组)和阴性对照组(sh-NC组), 检测转染效率。以β-actin作为加载对照, 测定上述细胞系中*ANLN* mRNA水平。数据显示为三个生物重复值的$\bar{x}\pm s$。采用双尾学生t检验确定统计学意义。*P<0.05, 与sh-NC组相比; D: Western blot分析。检测sh-*ANLN*组和sh-NC组的转染效率。以β-actin作为加载对照, 测定上述细胞系中ANLN蛋白水平。数据显示为三个生物重复值的$\bar{x}\pm s$。采用双尾学生t检验确定统计学意义。*P<0.05, 与sh-NC组相比。

A: ANLN overexpression was negatively correlated with survival in patients with GC. OS (overall survival) analysis; B: expression of ANLN in GC cells (SGC-7901 and MGC-803) and gastric normal cells GES-1. ANLN expression level in SGC-7901, MGC-803 and GES-1 cell lines was analyzed by Western blot analysis, **P<0.01 compared with GES-1 group; C: real-time PCR analysis. The lentivirus vector plasmid of pLenti-shRNA-*ANLN* and pLenti-shRNA-NC were respectively transfected into MGC-803 cells as experimental group (sh-*ANLN* group) and negative control (sh-NC group), the down-expression efficiency was detected. The relative *ANLN* mRNA expression level was normalized to β-actin. Data are shown as the $\bar{x}\pm s$ of the values from three independent experiments. Statistical significance was determined with a two-tailed Student's t-test. *P<0.05 compared with sh-NC group; D: Western blot analysis. The transfection efficiency of sh-*ANLN* group and sh-NC group was detected. β-actin was used as the loading control, and the ANLN protein levels in the above cell lines were quantified. Data are shown as the $\bar{x}\pm s$ of the values from three biological replicates. Statistical significance was determined with a two-tailed Student's t-test. *P<0.05 compared with sh-NC.

图1 ANLN在人胃癌中过表达且与胃癌预后相关

Fig.1 ANLN is abnormally overexpressed in GC cells and is associated with prognosis of GC

tion, we utilized wound healing assays and migration assays. The results revealed that cells with knockdown of *ANLN* expression had weaker migration capacity than cells transfected with control-shRNA (Fig.2A and Fig.2B). Next, we used Matrigel Trans-well assays to determine whether knockdown of *ANLN* expression affected MGC-803 human GC cells invasion, and the results showed that compared to sh-NC cells, cells with down-regulated of *ANLN* expression were less invasive (Fig.2C). MMPs can degrade almost all protein components in the ECM (extracellular matrix) to destroy the histological barrier of tumor cell invasion [30]. MMP2 and MMP9 expression after down-regulating *ANLN* expression were determined by Western blot assay, and the results showed that the two MMPs proteins decreased while *ANLN* silencing (Fig.2D). In conclusion, the above *in vitro* experiments can prove that ANLN may play a positive role in the metastasis of GC cells.

2.3 Depletion of *ANLN* blocks EMT in MGC-803 cells by devitalizing Smads

In order to explore the potential molecular signaling pathways that reduce the metastasis ability of human GC cells due to *ANLN* silencing, we examined the changes in EMT-related proteins in GC cells with *ANLN* silencing, and the results of Western blot assay showed that *ANLN* silencing significantly increased E-cadherin protein expression and reduced expression of N-cadherin and Vimentin protein, and that suppressed transcription factors Snail and Slug expression compared with sh-NC cells (Fig.3A). We next investigated whether Smads participate in the ANLN-mediated activation of EMT. Smad2, Smad3, p-Smad2 and p-Smad3 expression were detected by Western blot, and the resulted showed that *ANLN* silencing significantly reduced p-Smad2 and p-Smad3 expression (Fig.3B). Taken together, these results show that *ANLN* knockdown can inactivate Smad2 and Smad3 to block EMT.

2.4 ANLN regulates c-Myc via interactions with c-Myc in the nucleus, subsequently phosphorylating c-Myc to induce EMT without activating Smads

In order to explore other molecular mechanisms of EMT mediated by *ANLN* silencing in human GC cells, the expression levels of c-Myc and p-c-Myc in human GC cells were detected by Western blot assay, and the results showed that *ANLN* silencing significantly suppressed expression level of c-Myc and p-c-Myc (Fig.4A). Based on it, we hypothesized that ANLN could regulate phosphorylation of c-Myc by binding to c-Myc, thus activating EMT. To test this hypothesis, co-IF and co-IP assays were performed. We found an exact interaction between endogenous ANLN and endogenous c-Myc, and this binding was found in the nucleus, and *ANLN* silencing was accompanied by a reduction in the binding rate in the nucleus (Fig.4B and Fig.4C).

We also utilized a specific inhibitor (10058-F4) that targets both c-Myc and p-c-Myc to detect the role of c-Myc in the regulation of EMT by knocking out *ANLN*. E-cadherin, N-cadherin and Snail and Slug transcription factors expression levels were tested by Western blot assay, and we found 10058-F4 significantly increased E-cadherin expression and depressed N-cadherin expression level, and that remarkably decreased transcription factors Snail and Slug expression (Fig.5A). However, 10058-F4 treatment took no effect on Smad proteins (Fig.5A). Therefore, we assumed that phosphorylation of c-Myc via interactions with ANLN activates the expression of the above transcription factors to promote EMT without activating Smads. Therefore, our experiment using TGF-β to stimulate TGF-β signaling pathway just confirmed our conjecture. The Western blot assays showed that *ANLN* silencing inhibited EMT by suppressing crosstalk between independent Smads and c-Myc signaling pathways, and that was reversed by TGF-β treatment, which resulted in E-cadherin protein down-expression and N-cadherin protein over-expression (Fig.5B). Synthetically, our study showed that phosphorylation of c-Myc via interactions with ANLN activates the expression of downstream transcription factors (Snail and Slug), without activating Smads, to synergistically promote EMT.

3 Discussion

In this study, we demonstrated the roles of ANLN in MGC-803 human GC cells and determined

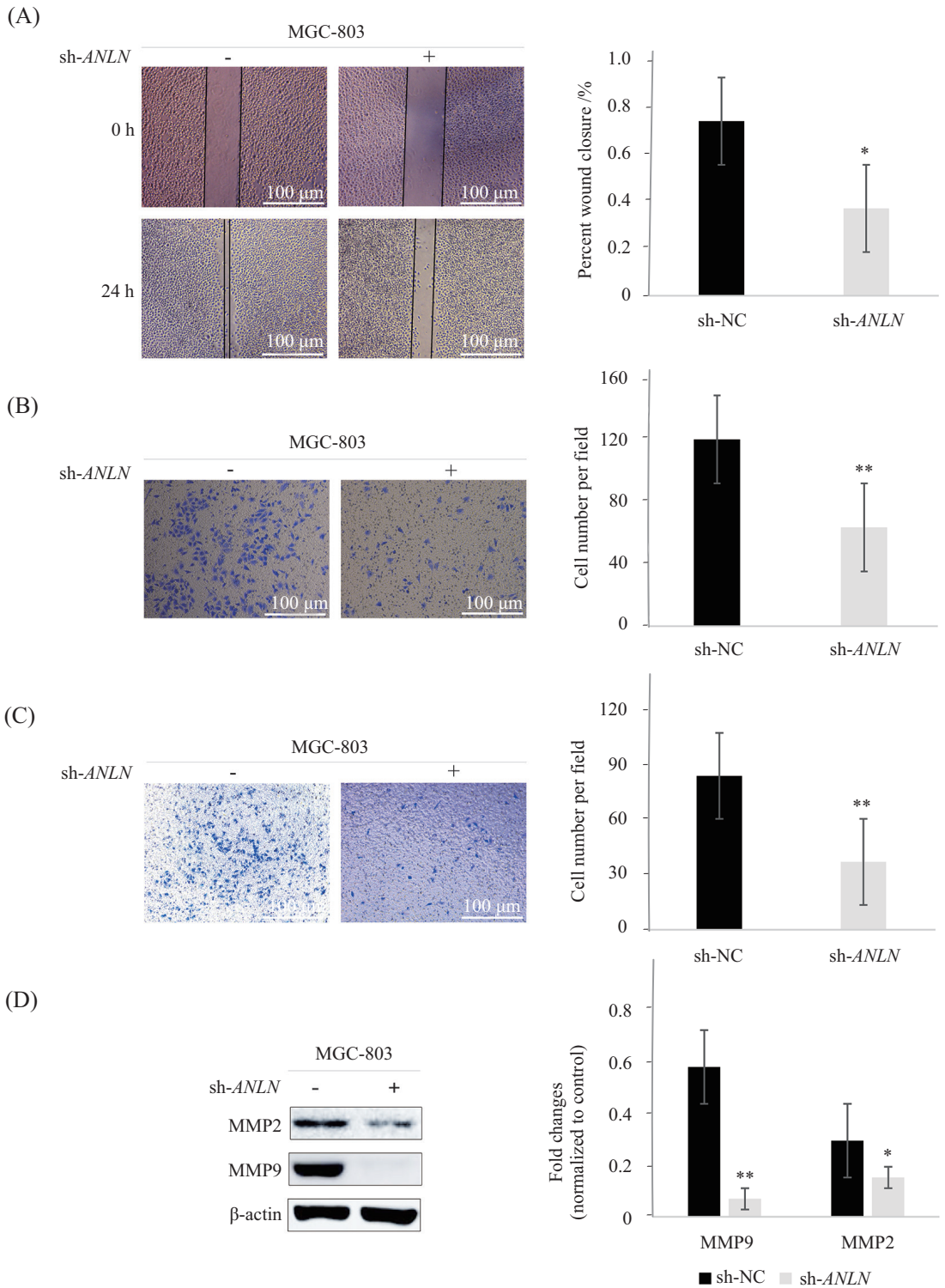

A: 伤口愈合实验, 计算创面愈合率; B: 跨孔Trans-well实验, 计算每个空间的细胞数; C: 基质Trans-well实验, 计算每个空间的细胞数; D: 采用Western blot检测MMP2和MMP9的表达水平。以β-actin为内参, 利用ImageJ软件分析条带蛋白的灰度值。所有数据代表三个生物重复值的$\bar{x}\pm s$。采用双尾学生t检验确定统计学意义。*P<0.05, **P<0.01, 与sh-NC组相比。

A: wound-healing assays. The wound closure rate was calculated; B: Trans-well migration assays. The cell number per field was calculated; C: matrigel Trans-well assays. The cell number per field was calculated; D: MMP2 and MMP9 expression levels were analyzed by Western blot assay. β-actin was used as the internal reference, and the gray level of stripe protein was analyzed by ImageJ software. All data represent the $\bar{x}\pm s$ of the values from three biological replicates. Statistical significance was determined with a two-tailed Student's t-test. *P<0.05, **P<0.01 compared with sh-NC group.

图2 体外沉默*ANLN*可抑制MGC-803细胞的迁移和侵袭

Fig.2 Depletion of *ANLN* inhibits the migration and invasion of MGC-803 cells *in vitro*

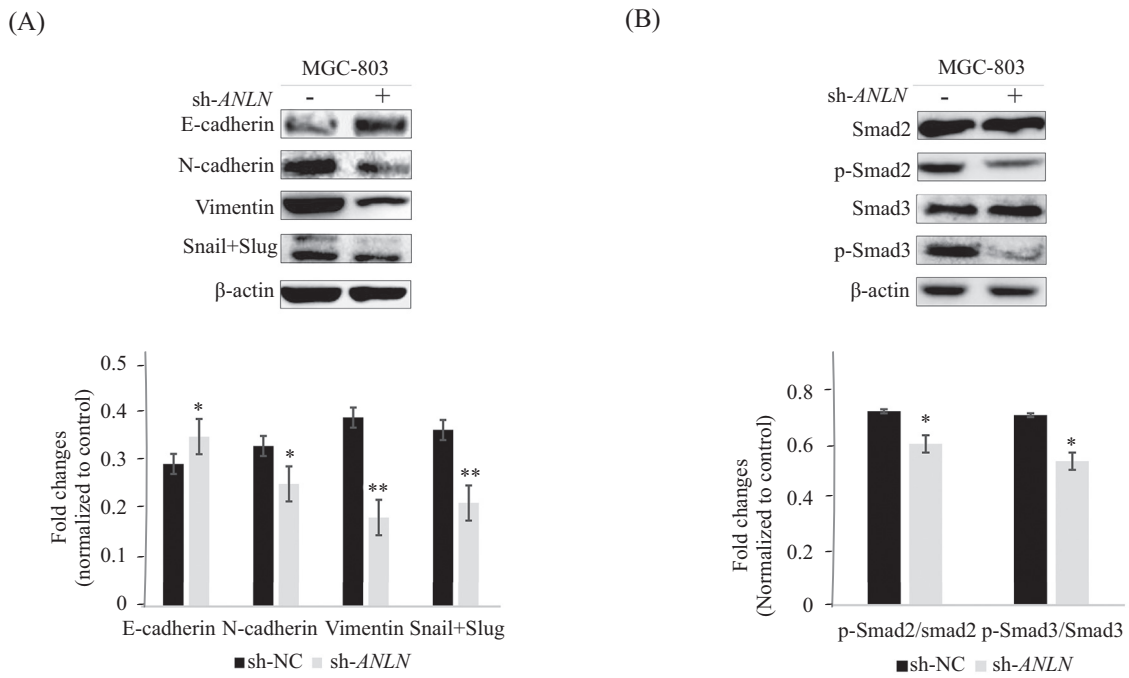

A: 采用Western blot检测E-cadherin、N-cadherin、Vimentin和Snail(Slug)的表达水平; B: 采用Western blot检测Smad2、Smad3、p-Smad2(S467)和p-Smad3(S423和S425)的表达水平。以β-actin为内参, 利用ImageJ软件分析条带蛋白的灰度值。所有数据代表三个生物重复值的$\bar{x}\pm s$。采用双尾学生*t*检验确定统计学意义。*P<0.05, **P<0.01, 与sh-NC组相比。

A: E-cadherin, N-cadherin, Vimentin and Snail (Slug) expression levels were analyzed by Western blot assay; B: Smad2, Smad3, p-Smad2 (S467) and p-Smad3 (S423 and S425) expression levels were analyzed by Western blot assay. β-actin was used as the internal reference, and the gray level of stripe protein was analyzed by ImageJ software. All data represent the $\bar{x}\pm s$ of the values from three biological replicates. Statistical significance was determined with a two-tailed Student's *t*-test. *P<0.05, **P<0.01 compared with sh-NC group.

图3　沉默*ANLN*可通过影响Smads的表达阻断MGC-803细胞EMT

Fig.3　Depletion of *ANLN* blocks EMT in MGC-803 cells by influencing Smads

the possible underlying mechanism. GC cell line was showed to have highly expression of ANLN, and the overexpressed ANLN contributed to the progression of GC. Furthermore, ANLN played a positive role in the metastasis of GC cells. At present, we determined by series of experiments *in vitro* that *ANLN* silencing inhibited metastasis behaviors of GC cells. We further showed that an exact interaction between endogenous ANLN and endogenous c-Myc, and knockout of *ANLN* was accompanied by a reduction in the binding rate in the nucleus. Additionally, c-Myc through its interaction with ANLN activated the expression of the transcription factors (Snail and Slug) to synergistically promote EMT without activating Smads. These findings represented a mechanism of ANLN promote EMT by interacting with c-Myc and mediating Smads respectively, and then targeting Snail and Slug downstream transcription factors; moreover, hyperactivation of EMT was shown to be associated with GC cell motility and invasion.

In this study, we showed that *ANLN* silencing effectively blocked EMT through the upregulation of E-cadherin expression and downregulation of N-cadherin and Vimentin expression in GC cells. In further experiments, we found that ANLN was positively correlated with the expression of EMT-related transcription factors (Snail and Slug). In conclusion, our results suggest that ANLN consumption attenuates EMT by downregulating the expression of EMT-related transcription factors. Additionally, MMPs, which are pathologically related to EMT, modify the ECM to enable cell motility and induce the expression of transcription factors associated with EMT to facilitate EMT [31-32]. In this study, we demonstrated that both MMP2 and MMP9 proteins were significantly decreased when EMT was attenuated by ANLN silencing, indicating that knockdown of

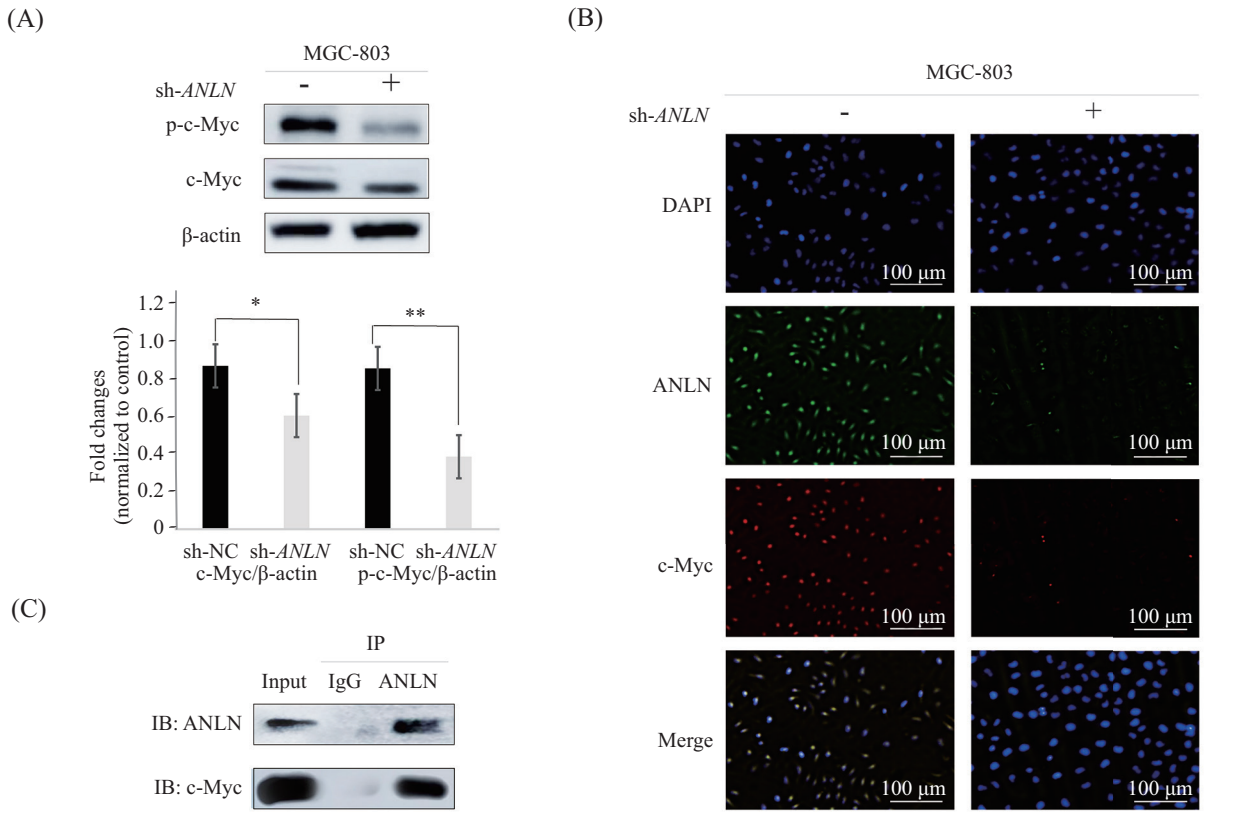

A: Western blot分析c-Myc 和p-c-Myc (S62)蛋白水平。实验采用β-actin作为内参, 采用ImageJ软件进行灰度分析, 所有数据代表三个生物重复值的$\bar{x}\pm s$。采用双尾学生t检验确定统计学意义。*P<0.05, **P<0.01, 与sh-NC组相比; B: ANLN和c-Myc 的共定位免疫荧光分析面板显示了三个实验中的一个的代表性图像; C: 免疫共沉淀Co-IP化验。转染细胞经ANLN抗体和c-Myc 抗体免疫沉淀检测洗脱蛋白的c-Myc, 分为实验组、裂解液组和IgG对照组。采用三次重复实验的平均值作为数据。

A: Western blot analysis of c-Myc and p-c-Myc (S62) protein levels. β-actin was used as the internal reference of this experiment, and ImageJ software was used for grayscale analysis. All data represent the $\bar{x}\pm s$ of the values from three biological replicates. Statistical significance was determined with a two-tailed Student's t-test. *P<0.05, **P<0.01 compared with sh-NC group; B: co-localization immunofluorescence analysis for ANLN and c-Myc. Panels show representative images from one of three experiments; C: Co-IP (co-immunoprecipitation) assays. The transfected cells were immunoprecipitated by ANLN antibody and c-Myc antibody was used to detect c-Myc of the eluted proteins. They were divided into experimental group, lysate group and IgG control group. The average of three independent experimental values was used as data.

图4 ANLN与c-Myc 相互作用触发MGC-803细胞的EMT

Fig.4 Interaction between ANLN and c-Myc triggers EMT in MGC-803 cells

ANLN potentially impairs the abovementioned MMP2 and MMP9 regulatory loop, thereby blocking EMT.

Next, we found that *ANLN* silencing decreased the phosphorylation of Smad2 and remarkably decreased the phosphorylation of Smad3 in MGC-803 cells, suggesting that *ANLN* knockdown blocks EMT by inhibiting p-Smad2 and p-Smad3. Additionally, TGF-β signaling pathway initiation upon TGF-β binding to TβRII and TβRI on the cell surface leads to TβRI phosphorylation by TβRII, and activation of TβRI further phosphorylates downstream the transcriptional factors Smad2 and Smad3 at two C terminal serine in the cytoplasm [33-34]. The Smad2 and Smad3 proteins binding to Smad4 to form Smads complex, which is then transferred to the nucleus to work with transcriptional coactivators or transcriptional corepressors in the nucleus to regulate transcription of target genes [33-34]. We found that knockdown of ANLN expression decreased activation of Smad2 and Smad3, thereby inhibiting EMT to some extent, which may be a supplement to the typical TGF-β-induced signaling pathway.

Myc and ANLN have been discovered to interact through experimental evidence, including affinity capture-MS [13], proximity label-MS [14] and curated by the Biogrid [15]. One important finding reported here is the cooperation of ANLN with c-Myc to induce

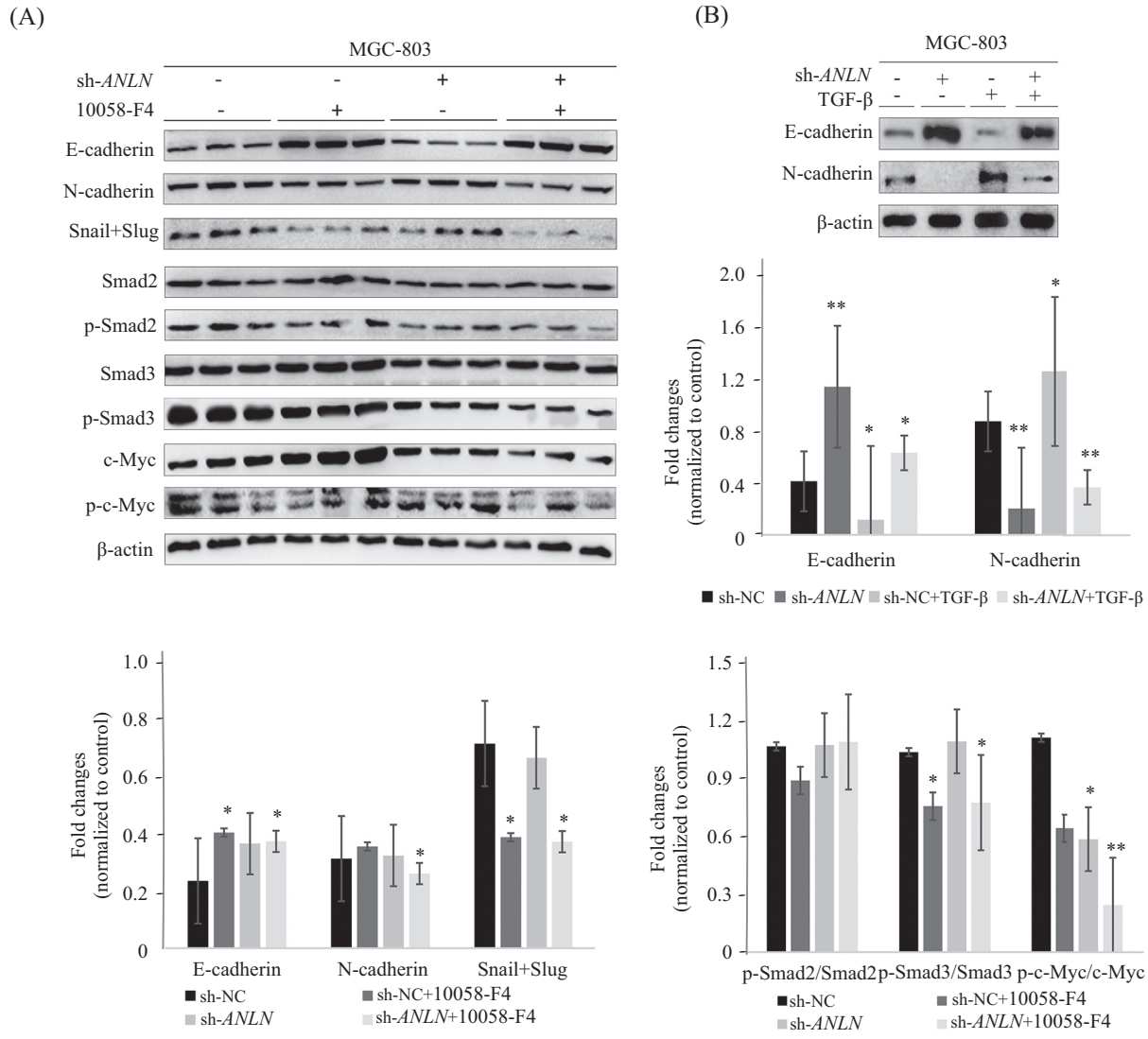

A: Western blot实验; 将细胞分为两组, 一组用10058-F4处理, 另一组不用10058-F4处理, 培养24 h后提取蛋白质。Western blot检测E-cadherin、N-cadherin、Snail(Slug)、Smad2、Smad3、p-Smad2(S467)、p-Smad3(S423和S425)、c-Myc 和p-c-Myc (S62)蛋白水平。实验采用β-actin作为内参, 采用ImageJ软件进行灰度分析。所有数据代表三个生物重复值的$\bar{x}\pm s$。采用双尾学生t检验确定统计学意义。*P<0.05, **P<0.01, 与sh-NC&无10058-F4组相比; B: 10 ng/mL TGF-β或不加TGF-β作用细胞24 h后提取蛋白。采用Western blot检测E-cadherin和N-cadherin的表达水平。实验采用β-actin作为内参, 采用ImageJ软件进行灰度分析。所有数据代表三个生物重复值的$\bar{x}\pm s$。采用双尾学生t检验确定统计学意义。*P<0.05, **P<0.01, 与sh-NC组相比。

A: Western blot assays. The cells were divided into two groups, one group was treated with 10058-F4 cells and the other group was not treated with 10058-F4 cells and cultured for 24 h. After the 24 h treatment, proteins were extracted. E-cadherin, N-cadherin, Snail (Slug), Smad2, Smad3, p-Smad2 (S467), p-Smad3 (S423 and S425), c-Myc and p-c-Myc (S62) protein levels were determined by Western blot assay. β-actin was used as the internal reference of this experiment, and ImageJ software was used for grayscale analysis. All data represent the $\bar{x}\pm s$ of the values from three biological replicates. Statistical significance was determined with a two-tailed Student's t-test. *P<0.05, **P<0.01 compared with sh-NC & no 10058-F4 group; B: cells were treated with or without 10 ng/mL TGF-β for 24 h. After the 24 h treatment, proteins were extracted. E-cadherin and N-cadherin expression levels were analyzed by Western blot assay. β-actin was used as the internal reference of this experiment, and ImageJ software was used for grayscale analysis. All data represent the $\bar{x}\pm s$ of the values from three biological replicates. Statistical significance was determined with a two-tailed Student's t-test. *P<0.05, **P<0.01 compared with sh-NC group.

图5 ANLN与c-Myc 相互作用触发MGC-803细胞的EMT但并不激活Smads蛋白

Fig.5 Interaction between ANLN and c-Myc triggers EMT in MGC-803 cells but does not activate Smads

EMT in MGC-803 human GC cells. From the present results, we found that ANLN activates the expression of transcription factors (Snail and Slug) through binding to c-Myc and subsequent phosphorylating c-Myc, promoting EMT without activating Smad proteins. c-Myc contains six highly conserved regions called

MBs (Myc homology boxes), in which MB0, MBI and MBII are located in the TAD (transcriptional activation domain) [16]. MB0 can not only act on tumor initiation, but also accelerate tumor growth. It directly binds to the general transcription factor TFIIF to mediate the interaction with the transcription extension factor. MBI contains T58 and S62 residues, which are phosphorylated to regulate Myc activity and stability [35-37]. MBII mediates interactions with acetyltransferase-containing complexes, enabling histone acetylation, and is essential for Myc -dependent tumor initiation [38-40]. We thereby speculated that MAX mediates the interaction of MBI with ANLN, and that phosphorylation of c-Myc at S62 activates the expression of the above transcription factors to promote EMT. This conjecture can also be extended to how MAX mediates the binding of c-Myc to ANLN, and how c-Myc is phosphorylated after binding to activate EMT signaling pathway. Therefore, further investigations are required to determine our conjecture.

In summary, we can understand the potential molecular mechanisms by which ANLN binds c-Myc and mediates independent Smads targeting downstream transcription factors to trigger EMT. In addition, we found that *ANLN* silencing and EMT is reversed by TGF-β, which activates the canonical TGF-β-induced signaling pathway to enhance the phosphorylation of Smad2 and Smad3 in the nucleus; this further confirmed the molecular mechanism of ANLN regulating EMT through direct binding with c-Myc protein and mediating Smads signaling pathway, respectively. Our study showed that ANLN is a crucial modulator of human GC metastasis. Furthermore, our study represented a possible molecular mechanism in which ANLN mediates independent Smads and c-Myc signaling pathways, which target Snail and Slug downstream transcription factors to trigger EMT. Our study indicated that ANLN may be a new therapeutic target for GC patients.

参考文献 (References)

[1] AJANI J A, D'AMICO T A, ALMHANNA K, et al. Gastric Cancer, Version 3.2016, NCCN Clinical Practice Guidelines in Oncology [J]. J Natl Compr Canc Netw, 2016, 14(10): 1286-312.

[2] SANO T. Gastric cancer: Asia and the world [J]. Gastric Cancer, 2017, 20(Suppl 1): 1-2.

[3] ZONG L, ABE M, SETO Y, et al. The challenge of screening for early gastric cancer in China [J]. Lancet, 2016, 388(10060): 2606.

[4] YOON H, KIM N. Diagnosis and management of high risk group for gastric cancer [J]. Gut Liver, 2015, 9(1): 5-17.

[5] PIEKNY A J, MADDOX A S. The myriad roles of Anillin during cytokinesis [J]. Semin Cell Dev Biol, 2010, 21(9): 881-91.

[6] HALL P A, TODD C B, HYLAND P L, et al. The septin-binding protein anillin is overexpressed in diverse human tumors [J]. Clin Cancer Res, 2005, 11(19 Pt 1): 6780-6.

[7] OLAKOWSKI M, TYSZKIEWICZ T, JARZAB M, et al. NBL1 and anillin (ANLN) genes over-expression in pancreatic carcinoma [J]. Folia Histochem Cytobiol, 2009, 47(2): 249-55.

[8] WANG A, DAI H, GONG Y, et al. ANLN-induced EZH2 upregulation promotes pancreatic cancer progression by mediating miR-218-5p/LASP1 signaling axis [J]. J Exp Clin Cancer Res, 2019, 38(1): 347.

[9] IDICHI T, SEKI N, KURAHARA H, et al. Regulation of actin-binding protein ANLN by antitumor miR-217 inhibits cancer cell aggressiveness in pancreatic ductal adenocarcinoma [J]. Oncotarget, 2017, 8(32): 53180-93.

[10] WANG G, SHEN W, CUI L, et al. Overexpression of Anillin (ANLN) is correlated with colorectal cancer progression and poor prognosis [J]. Cancer Biomark, 2016, 16(3): 459-65.

[11] MAGNUSSON K, GREMEL G, RYDEN L, et al. ANLN is a prognostic biomarker independent of Ki-67 and essential for cell cycle progression in primary breast cancer [J]. BMC Cancer, 2016, 16(1): 904.

[12] LONG X, ZHOU W, WANG Y, et al. Prognostic significance of ANLN in lung adenocarcinoma [J]. Oncol Lett, 2018, 16(2): 1835-40.

[13] HEIDELBERGER J B, VOIGT A, BORISOVA M E, et al. Proteomic profiling of VCP substrates links VCP to K6-linked ubiquitylation and c-Myc function [J]. EMBO Rep, 2018, 19(4): e44754.

[14] KALKAT M, RESETCA D, LOURENCO C, et al. Myc protein interactome profiling reveals functionally distinct regions that cooperate to drive tumorigenesis [J]. Mol Cell, 2018, 72(5): 836-48,e7.

[15] OUGHTRED R, STARK C, BREITKREUTZ B J, et al. The BioGRID interaction database: 2019 update [J]. Nucleic Acids Res, 2019, 47(D1): D529-D41.

[16] MEYER N, PENN L Z. Reflecting on 25 years with Myc [J]. Nat Rev Cancer, 2008, 8(12): 976-90.

[17] HOFFMAN B, LIEBERMANN D A. The proto-oncogene c-Myc and apoptosis [J]. Oncogene, 1998, 17(25): 3351-7.

[18] BLACKWOOD E M, EISENMAN R N. Max: a helix-loop-helix zipper protein that forms a sequence-specific DNA-binding complex with Myc [J]. Science, 1991, 251(4998): 1211-7.

[19] AMATI B, BROOKS M W, LEVY N, et al. Oncogenic activity of the c-Myc protein requires dimerization with Max [J]. Cell, 1993, 72(2): 233-45.

[20] SABO A, KRESS T R, PELIZZOLA M, et al. Selective transcriptional regulation by Myc in cellular growth control and lym-

phomagenesis [J]. Nature, 2014, 511(7510): 488-92.

[21] Correction to lancet infectious diseases 2020; published online April 29. https://doi.org/10.1016/ S1473-3099(20)30064-5 [J]. Lancet Infect Dis, 2020, 20(7): e148.

[22] HANRAHAN K, O'NEILL A, PRENCIPE M, et al. The role of epithelial-mesenchymal transition drivers ZEB1 and ZEB2 in mediating docetaxel-resistant prostate cancer [J]. Mol Oncol, 2017, 11(3): 251-65.

[23] WU C W, PENG M L, YEH K T, et al. Inactivation of p53 in pterygium influence miR-200a expression resulting in ZEB1/ZEB2 up-regulation and EMT processing [J]. Exp Eye Res, 2016, 146: 206-11.

[24] BLANCO M J, MORENO-BUENO G, SARRIO D, et al. Correlation of Snail expression with histological grade and lymph node status in breast carcinomas [J]. Oncogene, 2002, 21(20): 3241-6.

[25] MOLINA-ORTIZ P, VILLAREJO A, MACPHERSON M, et al. Characterization of the SNAG and Slug domains of Snail2 in the repression of E-cadherin and EMT induction: modulation by serine 4 phosphorylation [J]. PLoS One, 2012, 7(5): e36132.

[26] YANG J, MANI S A, DONAHER J L, et al. Twist, a master regulator of morphogenesis, plays an essential role in tumor metastasis [J]. Cell, 2004, 117(7): 927-39.

[27] LIU Y N, YIN J J, ABOU-KHEIR W, et al. MiR-1 and miR-200 inhibit EMT via Slug-dependent and tumorigenesis via Slug-independent mechanisms [J]. Oncogene, 2013, 32(3): 296-306.

[28] BRAEUTIGAM C, RAGO L, ROLKE A, et al. The RNA-binding protein Rbfox2: an essential regulator of EMT-driven alternative splicing and a mediator of cellular invasion [J]. Oncogene, 2014, 33(9): 1082-92.

[29] JIA H, YU F, LI B, et al. Actin-binding protein Anillin promotes the progression of gastric cancer *in vitro* and in mice [J]. J Clin Lab Anal, 2021, 35(2): e23635.

[30] COHEN M, WUILLEMIN C, IRION O, et al. Regulation of MMP-9 by p53 in first trimester cytotrophoblastic cells [J]. Hum Reprod, 2008, 23(10): 2273-81.

[31] NISTICO P, BISSELL M J, RADISKY D C. Epithelial-mesenchymal transition: general principles and pathological relevance with special emphasis on the role of matrix metalloproteinases [J]. Cold Spring Harb Perspect Biol, 2012, doi: 10.1101/cshperspect.a011908.

[32] RADISKY D C, LEVY D D, LITTLEPAGE L E, et al. Rac1b and reactive oxygen species mediate MMP-3-induced EMT and genomic instability [J]. Nature, 2005, 436(7047): 123-7.

[33] SHI Y, MASSAGUE J. Mechanisms of TGF-beta signaling from cell membrane to the nucleus [J]. Cell, 2003, 113(6): 685-700.

[34] GUPTA P, SRIVASTAVA S K. HER2 mediated de novo production of TGFbeta leads to SNAIL driven epithelial-to-mesenchymal transition and metastasis of breast cancer [J]. Mol Oncol, 2014, 8(8): 1532-47.

[35] PULVERER B J, FISHER C, VOUSDEN K, et al. Site-specific modulation of c-Myc cotransformation by residues phosphorylated *in vivo* [J]. Oncogene, 1994, 9(1): 59-70.

[36] SEARS R, NUCKOLLS F, HAURA E, et al. Multiple Ras-dependent phosphorylation pathways regulate Myc protein stability [J]. Genes Dev, 2000, 14(19): 2501-14.

[37] WELCKER M, ORIAN A, JIN J, et al. The Fbw7 tumor suppressor regulates glycogen synthase kinase 3 phosphorylation-dependent c-Myc protein degradation [J]. Proc Natl Acad Sci USA, 2004, 101(24): 9085-90.

[38] STONE J, DE LANGE T, RAMSAY G, et al. Definition of regions in human c-Myc that are involved in transformation and nuclear localization [J]. Mol Cell Biol, 1987, 7(5): 1697-709.

[39] WASYLISHEN A R, STOJANOVA A, OLIVERI S, et al. New model systems provide insights into Myc -induced transformation [J]. Oncogene, 2011, 30(34): 3727-34.

[40] MCMAHON S B, VAN BUSKIRK H A, DUGAN K A, et al. The novel ATM-related protein TRRAP is an essential cofactor for the c-Myc and E2F oncoproteins [J]. Cell, 1998, 94(3): 363-74.